Investigation on the phosphine-free synthesis of CdSe nanocrystals by cadmium precursor injection†

Jin Zhong Niu, Huaibin Shen, Hongzhe Wang, Weiwei Xu, Shiyun Lou, Zuliang Du and Lin Song Li*

Received (in Victoria, Australia) 22nd May 2009, Accepted 2nd July 2009
First published as an Advance Article on the web 10th August 2009
DOI: 10.1039/b9nj00212j

A green route for the synthesis of high quality zinc blende CdSe nanocrystals has been successfully established by using phosphine-free Se precursors combined with a cadmium precursor injection method. The effects of using different Se precursors, and adjustment of the molar ratios between the Cd and Se precursors have been investigated in detail to optimize the synthesis conditions. Absorption and photoluminescence (PL) spectra, X-ray diffraction (XRD), and transmission electron microscopy (TEM) were used for the characterization of synthesized CdSe nanocrystals. High brightness with the photoluminescence quantum yields up to 50% and narrow size-distribution with the full width at half-maximum (FWHM) below 24 nm were obtained under the optimized conditions. More than 5 g of high quality CdSe nanocrystals have been synthesized in one large scale reaction.

Introduction

Since the concept of the "size quantization effect" was introduced in the 1980s,[1] colloidal CdSe nanocrystals have become the most investigated object among inorganic semiconductor nanoparticles, partially because the emission color of CdSe nanocrystals spans almost all of the visible range. Using the attractive size-dependent optoelectronic properties, practical applications of CdSe nanocrystals in solar cells,[2,3] bioimaging,[4,5] sensors,[6–8] light-emitting diodes[9] and lasers[10,11] have been proposed. Many very successful preparation methods have been established for the synthesis of high quality CdSe nanocrystals, including the organometallic precursor route,[12–14] the alternative route,[15–19] the single molecule precursor route,[20–22] the microwave irradiation route,[23,24] *etc*. Most of these methods involve the use of alkylphosphines (such as trioctylphosphine (TOP) and tributylphosphine (TBP)) to prepare complex precursors between Se and TOP or TBP,[25–29] but TOP and TBP are hazardous, unstable and expensive materials, and generally a glove box is required for their use. With the concept of "green chemistry", some phosphine-free methods are welcomed as alternative routes to synthesize high quality CdSe nanocrystals. The Zou[30] and Mulvaney[31] groups have synthesized CdSe nanocrystals using elemental selenium dispersed in paraffin liquid or 1-octadecene (ODE), but the quality of the synthesized CdSe nanocrystals is not very good and only a small amount of CdSe nanocrystals was synthesized in their report.

Most recently, we have reported a "green" method to synthesize high quality CdSe nanocrystals using phosphine-free Se precursors.[32] In this previous work, a Se precursor solution was used as the injection solution. However, the solubility of Se in ODE is generally low, and the nucleation and growth stage of nanocrystals must be separated by the swift injection of precursors for the synthesis of high quality nanocrystals. As such, the volume of the Se precursors cannot be large, in order to facilitate the injection, and the amount of Se molecules that participate in the reaction is limited by the small volume of the Se injection solution. In this report, the Se powder was directly dissolved in ODE at elevated temperature to act as the reaction solution. CdO and oleic acid reacted in ODE to form Cd–OA complex solution, which acted as the injection solution. This is different from the traditional injection method, where the chalcogen precursors are usually used as the injection solution and the solution with the Cd precursors usually acts as the reaction solution, so our method was termed as the "inverse injection method". Using this approach, the Cd–OA complex has a high solubility in ODE, so the amount of Cd precursors injected into the reaction solution can be very large, which, together with the large amount of Se molecules dissolved in the large volume reaction solution, has led to the large scale synthesis of CdSe nanocrystals being conducted successfully. The effects of different Se precursors and Se : Cd molar ratios were investigated in detail to optimize the synthesis conditions. Three different Se precursors, Se–ODE, Se–OA–ODE and Se–ODA–ODE, were used for the synthesis of CdSe nanocrystals. Se : Cd molar ratios of 0.9 : 1, 1.8 : 1, 3.6 : 1, 7.5 : 1, 9.9 : 1 and 15 : 1 were tested. It was found that high quality CdSe nanocrystals were obtained with the Se : Cd molar ratios

Key Laboratory for Special Functional Materials of Ministry of Education, Henan University, Kaifeng 475004, P. R. China. E-mail: lsli@henu.edu.cn; Fax: +86 378-3881358; Tel: +86 378-3881358

† Electronic supplementary information (ESI) available: Temporal evolution of absorption spectra of synthesized CdSe nanocrystals using Se–OA–ODE and Se–ODA–ODE as the Se precursor. See DOI: 10.1039/b9nj00212j

of 7.5 : 1 and 9.9 : 1, and by using Se–ODE or Se–OA–ODE as the Se precursors.

Experimental section

All reagents were used as received without further experimental purification. Cadmium oxide (CdO, 99.99%, powder), selenium (Se, 99.99%, powder), 1-octadecene (ODE, 90%) and oleic acid (OA, 90%) were purchased from Aldrich. Hexanes (analytical grade), toluene (analytical grade) and methanol (analytical grade) were obtained from Beijing Chemical Reagent Ltd., China.

Solution of Cd precursor: the molar concentration of the Cd precursor was 0.1 mmol mL^{-1}. CdO (0.1284 g, 1 mmol), OA (0.846 g, 3 mmol) and ODE (9.05 mL) were loaded into a 25 mL three-neck flask, and heated to 240 °C under a nitrogen flow to obtain a clear colorless Cd precursor solution.

Stock solution of Se–ODE: the molar concentration of the Se–ODE precursor solution was 0.15 mmol mL^{-1}. 3 mmol (0.237 g) of Se powder was mixed with 20 mL of ODE, loaded into a 50 mL three-neck flask and degassed. The mixture was heated to 100 °C, maintained for 20 min, and subsequently heated to 220 °C and maintained for 3 h. During this period, the color of the mixture changed from transparent to orange and red, and finally turned yellow.

Stock solution of Se–OA–ODE: the molar concentration of the Se–OA–ODE precursor solution was 0.15 mmol mL^{-1}. 3 mmol (0.237 g) of Se powder was mixed with 9 mmol (2.538 g) OA and 17.8 mL of ODE, loaded into a 50 mL three-neck flask and degassed. The mixture was heated to 100 °C, maintained for 20 min, and subsequently heated to 220 °C and maintained for 3 h.

Stock solution of Se–ODA–ODE: the molar concentration of the Se–ODA–ODE precursor solution was 0.15 mmol mL^{-1}. 3 mmol (0.237 g) of Se powder was mixed with 9 mmol (2.426 g) ODA and 17.2 mL of ODE, loaded into a 50 mL three-neck flask and degassed. The mixture was heated to 100 °C, maintained for 20 min, and subsequently heated to 220 °C and maintained for 3 h.

In the series experiments of CdSe synthesis, for each reaction, 0.5 mL (0.05 mmol Cd–OA) of the Cd precursor injection solution was injected into the reaction solution composed of Se precursor solution and ODE solvent. The total volume of the reaction solution was kept at 5 mL. That means, when the molar ratios of Se : Cd changed from 0.9 : 1 to 1.8 : 1, 3.6 : 1, 7.5 : 1, 9.9 : 1 and 15 : 1, the composition of the reaction solution changed from 0.3 mL of Se precursor solution and 4.7 mL of ODE, 0.6 mL of Se precursor solution and 4.4 mL of ODE, 1.2 mL of Se precursor solution and 3.8 mL of ODE, 2.5 mL of Se precursor solution and 2.5 mL of ODE, 3.3 mL of Se precursor solution and 1.7 mL of ODE, and 5 mL of Se precursor solution, respectively. The reaction solution was heated to 280 °C under a nitrogen flow; at this temperature, 0.5 mL of Cd precursor solution was injected into the reaction solution, and then the temperature was reduced to 260 °C for nanocrystal growth. Aliquots were taken at different time intervals, and UV-vis and photoluminescence (PL) spectra were recorded for each aliquot. The synthesized CdSe nanocrystals could be dissolved in organic solvents like hexanes and toluene.

The samples used for optical measurements were prepared without any size sorting. UV-vis absorption spectra and PL spectra were recorded using an Ocean Optics spectrophotometer (mode PC2000-ISA). PL spectra were taken using an excitation wavelength of 365 nm. PL quantum yields (QYs) of nanocrystals were measured relative to coumarin 540 (QY = 78% in ethanol) and rhodamine 590 (QY = 95% in methanol). All the QY data of nanocrystals and dyes were collected through SPEX F212. The optical density (OD) values of the nanocrystal samples at the excitation wavelength were in the range of 0.02–0.05. X-Ray diffraction (XRD) studies of nanocrystals were carried out at room temperature with a Philips X' Pert Pro X-ray diffractometer using Cu Kα radiation (λ = 1.54 Å). Transmission electron microscopy (TEM) studies were performed using a Jeol JEM-100CX II microscope. TEM samples were prepared by placing a drop of the nanocrystal solution onto a 400 mesh carbon covered copper grid.

Results and discussion

In this report, firstly, a series of experiments were conducted to investigate the influence of different Se precursors and reagent molar ratios on the qualities of as-prepared CdSe nanocrystals in order to optimize the synthesis conditions. Fig. 1 shows the temporal evolution growth processes of CdSe nanocrystals using the three kinds of Se precursors, with Se : Cd molar ratios of 7.5 : 1 and 9.9 : 1. The absorption spectra were vertically offset for clarity and the PL spectra were normalized for clarity. As shown in Fig. 1, when using Se–ODE or Se–OA–ODE as the Se precursor, CdSe nanocrystals could grow to larger sizes compared with using the Se–ODA–ODE precursor, as indicated by a red-shift of PL peaks to over 600 nm. Their qualities were also better, as indicated by the observation of less than 30 nm full width at half-maximum (FWHM), compared with as broad as 40 nm FWHM by using Se–ODA–ODE as the precursor. At least three excitonic absorption features appeared in almost every absorption spectrum. Only at the very early stage of CdSe nanocrystal growth (the samples obtained before 10 s under every condition), did the unavoidable trap emission centered at ~650 nm appear. The band-gap PL of as-prepared CdSe nanocrystals synthesized using Se–OA–ODE as the Se precursor span from 490 to 640 nm, almost covering the visible range. When Se–ODA–ODE was used as the Se precursor, the CdSe nanocrystals did not easily grow to large sizes and the quality was poor, as indicated by fewer excitonic absorption features and most of the PL spectra with trap emissions centered at ~650 nm. The size distribution was broad for CdSe nanocrystals synthesized using Se–ODA–ODE precursors, indicated by the larger FWHM compared with CdSe nanocrystals synthesized using Se–ODE and Se–OA–ODE precursors, as shown in Fig. 2.

The growth speed of a nanocrystal is mainly determined by the crystal size and the monomers supplied to the nascent nanocrystal,[33] or it can be say, that the growth speed of nanocrystals in solution is determined by the difference of chemical potential between the crystal surface and the monomers.[34] In realistic experiments, the growth speed of

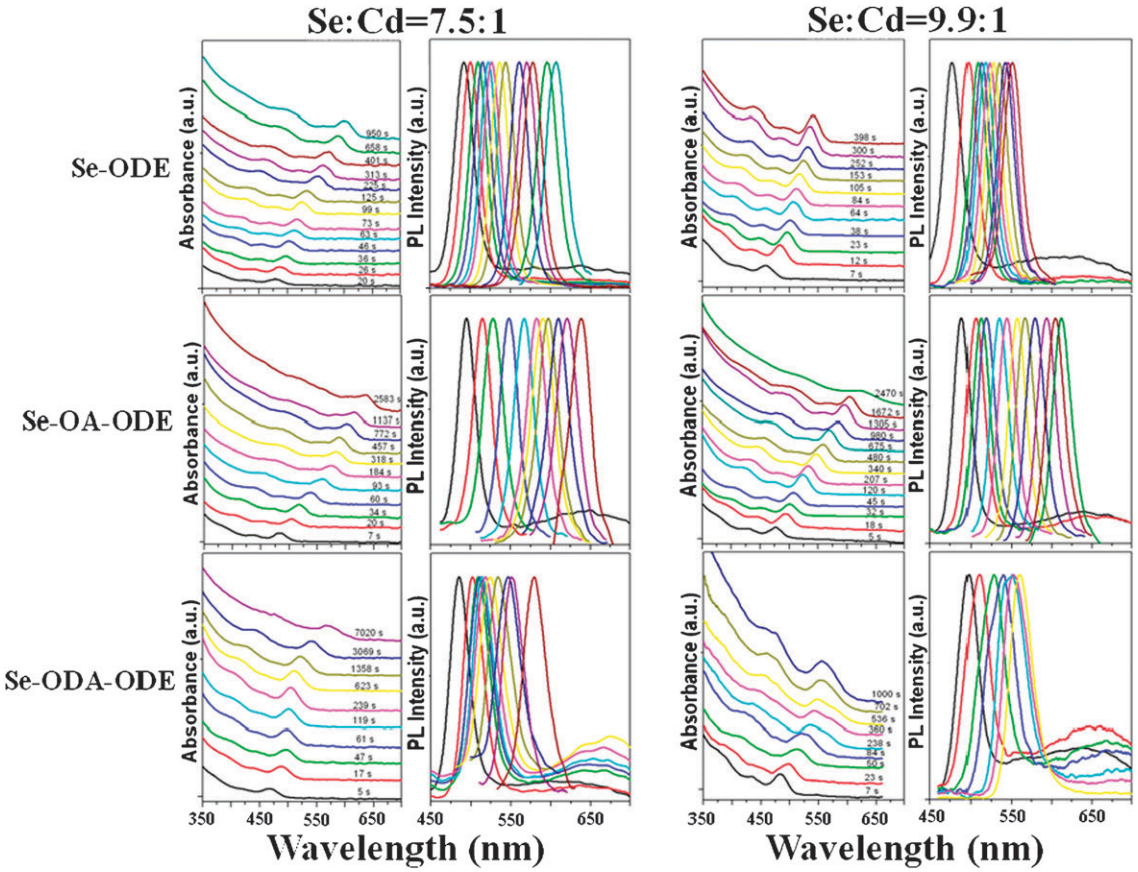

Fig. 1 The temporal evolution of absorption spectra and PL spectra of CdSe nanocrystals using different Se precursors (Se–ODE, Se–OA–ODE and Se–ODA–ODE, respectively) with the Se : Cd molar ratios of 7.5 : 1 and 9.9 : 1. With the use of the Se–ODA–ODE precursor, trap emissions appeared at about 650 nm in most of the spectra. The fractions of CdSe nanocrystals were diluted to a similar absorption intensity for the measurements. Note that the spectra are normalized and shifted for clarity.

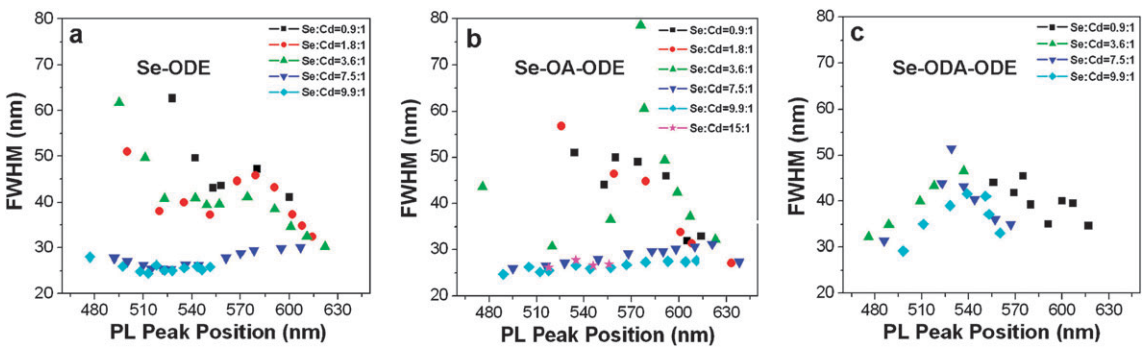

Fig. 2 The relationship between the FWHM of CdSe nanocrystals and their corresponding PL peak positions with different Se : Cd molar ratios using Se–ODE (a), Se–OA–ODE (b), and Se–ODA–ODE (c) precursors. The concentration of the Cd precursor was 0.0091 mmol mL^{-1} and kept same in all the reactions. When the Se : Cd molar ratios changed from 0.9 : 1, to 1.8 : 1, 3.6 : 1, 7.5 : 1, 9.9 : 1 and 15 : 1, the concentrations of the Se precursor changed from 0.0082 to 0.0164, 0.0327, 0.0682, 0.09 and 0.136 mmol mL^{-1}, respectively. All the reactions were conducted with an injection temperature of 280 °C and a growth temperature of 260 °C.

the ensemble of nanocrystals in the reaction solution is affected by many factors; in particular, the number of nuclei formed in the nucleation stage would strongly affect the growth speed in the growth stage of nanocrystals. If more nuclei are formed in the nucleation stage, there are fewer residual monomers, and the monomer supply in the growth stage cannot afford a quick growth and *vice versa*. Shown in Fig. 3 are the relationships between PL peak positions and the nanocrystal growth times (the injection time is the time started). Since the band-gap PL peak position is determined by the nanocrystal size in the size quantization region, Fig. 3 roughly reflects the growth rate of CdSe nanocrystals in different conditions. Fig. 3 compares the growth rate of CdSe nanocrystals when different Se precursors were used under the

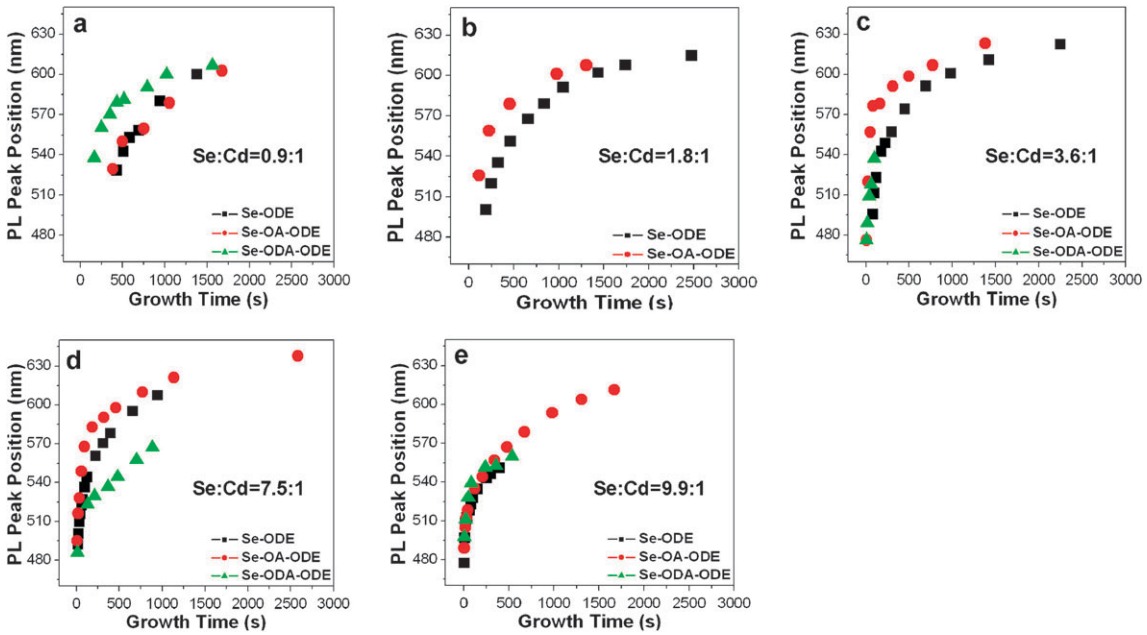

Fig. 3 The relationship between PL peak positions and the growth time of the CdSe nanocrystals using different Se precursors with Se : Cd molar ratios of 0.9 : 1 (a), 1.8 : 1 (b), 3.6 : 1 (c), 7.5 : 1 (d) and 9.9 : 1 (e). The concentration of the Cd precursor was 0.0091 mmol mL^{-1} and kept same in all of the reactions. The concentrations of the Se precursor changed from 0.0082 (a) to 0.0164 (b), 0.0327 (c), 0.0682 (d) and 0.09 mmol mL^{-1} (e). All the reactions were conducted with injection an temperature of 280 °C and a growth temperature of 260 °C.

same Se : Cd molar ratio. In every comparison, only the Se precursors were different; the amounts of Se and Cd, the volume of the reaction solution, the Se : Cd molar ratios and the injection/growth temperatures were all the same. In the comparison of the growth speed, if there are more nuclei formed in the nucleation stage, then more monomers are consumed in the nucleation stage, so fewer residual monomers are left in the reaction solution, and the monomer supply in the growth stage may be not enough to maintain a fast growth and so the growth speed is low. With the Se : Cd molar ratios of 3.6 : 1, 7.5 : 1 and 9.9 : 1, the fastest growth speed of CdSe nanocrystals in the early growth stage is obtained when Se–OA–ODE is used as the Se precursor, and the slowest growth speed is obtained when Se–ODA–ODE is used. This is in accordance with the previous results that more OA molecules restricted the nucleation of nanocrystals because the stronger complexation with Cd species,[18] the more residual monomers accelerated the growth of CdSe nanocrystals. For the use of Se–ODA–ODE, because the activation of Cd–OA complex by the ODA molecules,[25] more nuclei were formed in the nucleation stage, less residual monomers could not afford the fast growth of CdSe nanocrystals. As shown in Fig. 3, under almost all the Se : Cd molar ratios, CdSe nanocrystals synthesized using Se–OA–ODE always have the biggest size through the growth stage, compared with the use of Se–ODE and Se–ODA–ODE precursors. This substantially demonstrates that the existence of more OA molecules in the reaction system limited the nucleation of CdSe nanocrystals, and the more sufficient residual monomer supply can afford the fast nanocrystal growth. This is in accordance with our previous results that more OA molecules favor the growth of large-sized CdSe nanocrystals using the traditional Se precursor injection solution.[32]

It was clear that the band-gap emission of CdSe nanocrystals could be detected even below 490 nm using all three types of Se precursors with the Se : Cd molar ratios of 7.5 : 1 and 9.9 : 1. However, only PL peaks at 510 nm and higher could be detected when the Se : Cd molar ratios were 0.9 : 1 and 1.8 : 1 in all the three types of Se precursors (except the Se : Cd molar ratio of 1.8 : 1 using Se–ODA–ODE as the Se precursor; no PL signal was detected). If the molar ratio of Se : Cd was 15 : 1, only the use of Se–OA–ODE could produce CdSe nanocrystals with band-gap emissions, though the PL was only detected before 136 s (PL peak at 555 nm). Maybe under this condition, the growth was too fast and the good size-distribution was destroyed; such quick growth would destroy the quality of the nanocrystal surfaces, so the photogenerated excitons would relax through nonirradiation surface defects [35] and the band-gap emission could not be detected any more. The absorption spectra are shown in Fig. S1 in the ESI.† A similar result was obtained when Se–ODA–ODE was used as the Se precursor with the Se : Cd molar ratio of 15 : 1; no emissions appeared even though absorption spectra were relatively good. When Se–ODE was used as the Se precursor with the Se : Cd molar ratio of 15 : 1, neither absorption nor PL was detectable.

The temporal evolution of FWHM of as-synthesized CdSe nanocrystals using different Se precursors and under different Se : Cd molar ratios are shown in Fig. 2. FWHM is usually used as a guide to measure the quality of nanocrystals because it reflects their size-distribution; a narrow FWHM means a narrow size-distribution. The quality of the CdSe nanocrystals was not well controlled when Se–ODA–ODE was used as the Se precursor (Fig. 2c), the FWHM was usually above 30 nm, *i.e.* a broad size-distribution. When Se–ODE and Se–OA–ODE were used as the Se precursors, the quality of

synthesized CdSe nanocrystals was well controlled. With the Se : Cd molar ratios of 7.5 : 1 and 9.9 : 1, the FWHM was almost always under 30 nm, and as narrow as 24 nm was obtained. This indicates that the as-synthesized CdSe nanocrystals had a very narrow size-distribution.

The size-distribution focusing and defocusing phenomena with the use of Se–ODE as the Se precursor are shown in Fig. 2a. Under the Se : Cd molar ratios of 7.5 : 1 and 9.9 : 1, right after the injection of Cd precursors, the size-distribution focusing occurred until the CdSe nanocrystal grew to a size with the PL peak at 520 nm. After that, size-distribution defocusing occurred, meaning that Ostwald ripening happened, and the FWHM increased as the reaction proceed, until the end of the reaction. This fitted well with the theory reported by Peng *et al.*[36] However, with the Se : Cd molar ratios of 0.9 : 1, 1.8 : 1 and 3.6 : 1 using Se–ODE as the precursor, the situation is different. The size-distributions also focused after the injection of Cd precursors until the CdSe nanocrystals grew to a size with PL peaks at 550 nm, then, size-distribution defocusing occurred, and the FWHM broadened until the CdSe nanocrystals grew to a size with PL peaks at 580 nm. After that, however, it is interesting that the size-distribution refocusing occurred until the end of the reaction, with the final FWHM of about 30 nm in all the three cases with Se : Cd molar ratios of 0.9 : 1, 1.8 : 1 and 3.6 : 1, without the additional injection of precursors. Peng *et al.* reported that additional injection of precursors induced the size-distribution refocusing during the Ostwald ripening,[36] but in our results, size-distribution refocusing happened without additional precursor injection. In a previous report, size-distribution focusing also occurred in the Ostwald ripening stage by Monte Carlo simulation methods,[33] but that occurred in the situation with a broad size-distribution at the beginning of Ostwald ripening. In our results, the size-distribution refocusing phenomenon without additional injection of precursors in the middle stage of Ostwald ripening is very difficult to understand. Recently, Thessing *et al.* reported that maybe the interparticle interactions would impact the size-distribution of nanocrystals in solution, and the rapid and complete dissolution of small nanocrystals would result in focusing the size-distribution of the large size nanocrystals in the Ostwald ripening stage.[37] Maybe the dissolution of small CdSe nanocrystals produced much more monomers in the defocusing stage, just like the additional injection of precursors, caused the refocusing phenomenon in the following stage, but this needs further investigation. Size-distribution refocusing during the Ostwald ripening stage also occurred by using Se–OA–ODE as the Se precursor with the Se : Cd molar ratios of 0.9 : 1, 1.8 : 1 and 3.6 : 1. By using Se–ODA–ODE as the Se precursor, the size-distributions were large and disordered, indicating that the quality of synthesized CdSe nanocrystals was not good.

CdSe nanocrystals synthesized using all the three different Se precursors under different Se : Cd molar ratios have the same zinc blende crystal structure. The Se precursors may determine the crystal structure of the CdSe nanocrystals. Wurtzite-structured CdSe nanocrystals were always obtained when TBP–Se and TOP–Se were used as Se precursors. In a previous report by Mulvaney group, wurtzite-structured CdSe nanocrystals were also synthesized using phosphine-free

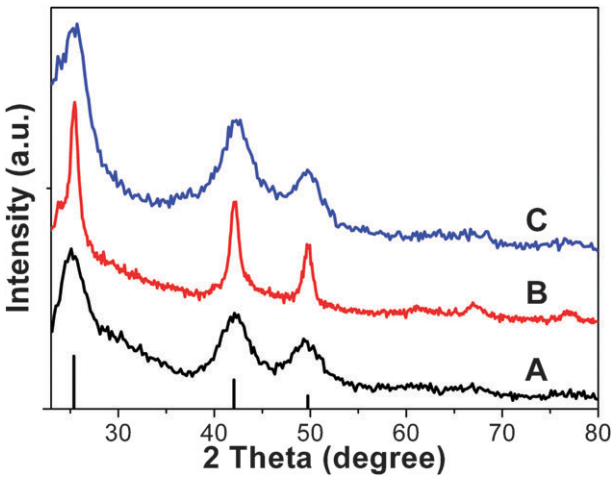

Fig. 4 XRD patterns of synthesized CdSe nanocrystals by the use of Se precursors of Se–ODE (A), Se–OA–ODE (B), and Se–ODA–ODE (C) with the Se:Cd molar ratio of 7.5 : 1.

Se–ODE precursors and they argued that the TMPPA molecules determined the crystal structures.[31] However, only zinc blende CdSe nanocrystals were obtained when phosphine-free Se precursors were used in our syntheses, in the Se injection precursor[32] or current inverse Cd injection precursor methods. The zinc blende structure facilitates the doping of nanocrystals.[38] Fig. 4 shows the typical X-ray diffraction patterns of as-prepared CdSe nanocrystals using different Se precursors. The peaks match well with the standard zinc blende structure of CdSe crystals. According to Scherrer's formula, crystallite size $t = K\lambda/(B \cos \theta)$, where K is the Scherrer constant, λ is the wavelength (1.54 Å for Cu Kα radiation), B is the FWHM of the XRD peak and θ is the peak position. For a perfect bulk crystal, the size is infinite and the B value will be zero, so the diffraction patterns are lines. When the crystal becomes smaller in size, B will have a larger value. The peaks in our XRD patterns show broadening phenomena because the synthesized CdSe nanocrystals are all below 10 nm. Shown in Fig. 5 are the typical TEM images of synthesized CdSe nanocrystals using different Se precursors. The narrow size-distributions of the samples are clearly

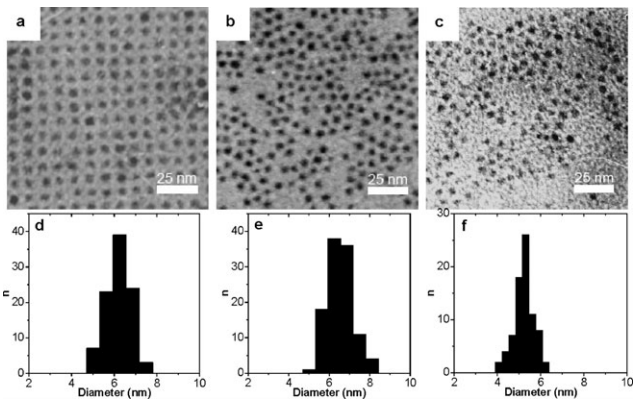

Fig. 5 TEM images of synthesized CdSe nanocrystals by the use of Se precursors: Se–ODE (a), Se–OA–ODE (b), and Se–ODA–ODE (c), respectively. d, e, and f are the corresponding size-distribution histograms obtained from the TEM image a, b, and c, respectively.

demonstrated by the corresponding histograms. The average diameters are 6.20 (d), 6.53 (e) and 5.23 nm (f), after calculating 96 (a), 108 (b) and 78 (c) isolated nanocrystals, respectively. It also shows the nanocrystals self-assembled into ordered close packed arrays, although no attempt was made to optimize the conditions for self-assembly.

The highest QYs of synthesized CdSe nanocrystals under optimized conditions were between 50–60% according to the method reported by Williams *et al*.[39] The brightness of CdSe nanocrystals synthesized by the inverse injection method here was as high as that of the best quality CdSe nanocrystals synthesized by the Se injection precursors reported before.[32] Using Se–ODE or Se–OA–ODE as the Se precursor, and Cd–OA as the injection solution, a large scale synthesis of CdSe nanocrystals could be easily conducted. More than 5 g of high quality CdSe nanocrystals were easily obtained in one synthesis using this inverse injection method. The largely reduced material cost and highly improved synthesis scale make this method especially useful in industrial applications.

Conclusions

In conclusion, CdSe nanocrystals have been successfully synthesized with the inverse injection method using three types of "green" phosphine-free Se precursors. High quality CdSe nanocrystals were obtained using Se–ODE and Se–OA–ODE as Se precursors with the Se : Cd molar ratios of 7.5 : 1 and 9.9 : 1. The synthesized CdSe nanocrystals span almost all of the visible range, and the narrowest FWHM was less than 24 nm with a quantum yield more than 50%. With these "green", low cost precursors, combined with the inverse injection method, the total cost of the syntheses of CdSe nanocrystals can be largely decreased 50% or more.

Acknowledgements

This work was supported by the research project of the National Natural Science Foundation of China (20771035), Hi-Tech Research and Development Program of China (863 plan, 2006AA03Z3592), Innovation Scientists and Technicians Troop Construction Projects of Henan Province, and the Scientific Research Foundation for the Returned Overseas Chinese Scholars, State Education Ministry.

References

1 L. E. Brus, *J. Chem. Phys.*, 1984, **80**, 4403–4409.
2 W. U. Huynh, X. Peng and A. P. Alivisatos, *Adv. Mater.*, 1999, **11**, 923–927.
3 I. Gur, N. A. Fromer, M. L. Geier and A. P. Alivisatos, *Science*, 2005, **310**, 462–465.
4 X. Gao, Y. Cui, R. M. Levenson, L. W. K. Chung and S. Nie, *Nat. Biotechnol.*, 2004, **22**, 969–976.
5 B. Dubertret, P. Skourides, D. J. Norris, V. Noireaux, A. H. Brivanlou and A. Libchaber, *Science*, 2002, **298**, 1759–1762.
6 R. C. Somers, M. G. Bawendi and D. G. Nocera, *Chem. Soc. Rev.*, 2007, **36**, 579–591.
7 P. T. Snee, R. C. Somers, G. Nair, J. P. Zimmer, M. G. Bawendi and D. G. Nocera, *J. Am. Chem. Soc.*, 2006, **128**, 13320–13321.
8 Y. S. Liu, Y. Sun, T. Vernier, C. H. Liang, S. Y. C. Chong and M. A. Gundersen, *J. Phys. Chem. C*, 2007, **111**, 2872–2878.
9 M. A. Schreuder, J. D. Gosnell, N. J. Smith, M. R. Warnement, S. M. Weiss and S. J. Rosenthal, *J. Mater. Chem.*, 2008, **18**, 970–975.
10 H. J. Eisler, V. C. Sundar, M. G. Bawendi, M. Walsh, H. I. Smith and V. Klimov, *Appl. Phys. Lett.*, 2002, **80**, 4614–4616.
11 Y. Chan, J. M. Caruge, P. T. Snee and M. G. Bawendi, *Appl. Phys. Lett.*, 2004, **85**, 2460–2462.
12 C. B. Murray, D. J. Norris and M. G. Bawendi, *J. Am. Chem. Soc.*, 1993, **115**, 8706–8715.
13 M. L. Steigerwald, A. P. Alivisatos, J. M. Gibson, T. D. Harris, R. Kortan, A. J. Muller, A. M. Thayer, T. M. Duncan, D. C. Douglass and L. E. Brus, *J. Am. Chem. Soc.*, 1988, **110**, 3046–3050.
14 J. Hambrock, A. Birkner and R. A. Fischer, *J. Mater. Chem.*, 2001, **11**, 3197–3201.
15 Z. A. Peng and X. Peng, *J. Am. Chem. Soc.*, 2001, **123**, 183–184.
16 L. Qu, Z. A. Peng and X. Peng, *Nano Lett.*, 2001, **1**, 333–337.
17 P. S. Nair, K. P. Fritz and G. D. Scholes, *Chem. Commun.*, 2004, 2084–2085.
18 W. W. Yu and X. G. Peng, *Angew. Chem., Int. Ed.*, 2002, **41**, 2368–2371.
19 C. R. Bullen and P. Mulvaney, *Nano Lett.*, 2004, **4**, 2303–2307.
20 M. Green and P. O'Brien, *Chem. Commun.*, 1999, 2235–2241.
21 S. L. Cumberland, K. M. Hanif, A. Javier, G. A. Khitrov, G. F. Strouse, S. M. Woessner and C. S. Yun, *Chem. Mater.*, 2002, **14**, 1576–1584.
22 D. J. Crouch, P. O'Brien, M. A. Malik, P. J. Skabara and S. P. Wright, *Chem. Commun.*, 2003, 1454–1455.
23 Q. Wang and D. K. Seo, *Chem. Mater.*, 2006, **18**, 5764–5767.
24 J. Zhu, O. Palchik, S. Chen and A. Gedanken, *J. Phys. Chem. B*, 2000, **104**, 7344–7347.
25 L. S. Li, N. Pradhan, Y. Wang and X. Peng, *Nano Lett.*, 2004, **4**, 2261–2264.
26 J. Joo, H. B. Na, T. Yu, J. H. Yu, Y. W. Kim, F. Wu, J. Z. Zhang and T. Hyeon, *J. Am. Chem. Soc.*, 2003, **125**, 11100–11105.
27 J. H. Warner and R. D. Tilley, *Adv. Mater.*, 2005, **17**, 2997–3001.
28 Y. Cheng, Y. Wang, F. Bao and D. Chen, *J. Phys. Chem. B*, 2006, **110**, 9448–9451.
29 P. D. Cozzoli, L. Manna, M. L. Curri, S. Kudera, C. Giannini, M. Striccoli and A. Agostiano, *Chem. Mater.*, 2005, **17**, 1296–1306.
30 Z. Deng, L. Cao, F. Tang and B. Zou, *J. Phys. Chem. B*, 2005, **109**, 16671–16675.
31 J. Jasieniak, C. Bullen, J. V. Embden and P. Mulvaney, *J. Phys. Chem. B*, 2005, **109**, 20665–20668.
32 H. Shen, H. Wang, Z. Tang, J. Z. Niu, S. Lou, Z. Du and L. S. Li, *CrystEngComm*, 2009, **11**, 1733–1738.
33 D. V. Talapin, A. L. Rogach, M. Haase and H. Weller, *J. Phys. Chem. B*, 2001, **105**, 12278–12285.
34 H. S. Chen and R. V. Kumar, *J. Phys. Chem. C*, 2009, **113**, 31–36.
35 D. V. Talapin, A. L. Rogach, E. V. Shevchenko, A. Kornowski, M. Haase and H. Weller, *J. Am. Chem. Soc.*, 2002, **124**, 5782–5790.
36 X. Peng, J. Wickham and A. P. Alivisatos, *J. Am. Chem. Soc.*, 1998, **120**, 5343–5344.
37 J. Thessing, J. Qian, H. Chen, N. Pradhan and X. Peng, *J. Am. Chem. Soc.*, 2007, **129**, 2736–2737.
38 S. C. Erwin, L. Zu, M. I. Haftel, A. L. Efros, T. A. Kennedy and D. J. Norris, *Nature*, 2005, **436**, 91–94.
39 A. T. R. Williams, S. A. Winfield and J. N. Miller, *Analyst*, 1983, **108**, 1067–1071.